

## Spin Correlations of 2D Quantum Antiferromagnet at Low Temperatures and a Direct Comparison with Neutron-Scattering Experiments

Hong-Qiang Ding and Miloje S. Makivić

Concurrent Computation Program and Physics Department, California Institute of Technology,  
Pasadena, California 91125

(Received 22 November 1989)

Correlation functions of the spin- $\frac{1}{2}$  2D Heisenberg antiferromagnet at low temperatures are computed via a large-scale Monte Carlo simulation on  $128 \times 128$  lattices. The correlation length is found to be accurately described by the exponentially divergent form typical of classical Heisenberg spins in two dimensions. The large correlation lengths measured are directly compared with the neutron-scattering experiments on  $\text{La}_2\text{CuO}_4$ . The excellent fit provides a first-principles determination of the exchange coupling:  $J = 1450 \pm 30$  K.

PACS numbers: 75.10.Jm, 74.70.Hk, 75.40.Mg

The discovery of high- $T_c$  superconductors<sup>1</sup> has brought about a resurgence of interest in two-dimensional (2D) quantum antiferromagnets. This follows from both theoretical<sup>2</sup> and experimental<sup>3,4</sup> indications that spin fluctuations play a significant role in the new mechanism for the high- $T_c$  superconductivity. The undoped compound  $\text{La}_2\text{CuO}_4$  exhibits a rich magnetic structure, which is considered to be well modeled by the spin- $\frac{1}{2}$  antiferromagnetic Heisenberg model (AFHM):

$$H = J \sum_{\langle ij \rangle} S_i \cdot S_j, \quad (1)$$

where  $\langle ij \rangle$  goes over all the nearest-neighbor pairs on the square lattice and  $S_i$  is the spin operator. The energy scale of the system is set by the exchange coupling  $J$ .

A considerable amount of work has been devoted to the study of this model. It is difficult to capture the highly quantum nature of spin- $\frac{1}{2}$  magnets.<sup>5</sup> Analytic studies based upon perturbative expansions have made important progress,<sup>5-8</sup> but so far crucial tests are still lacking. Given enough computing power, numerical methods can provide reliable quantitative results. In particular, finite-temperature Monte Carlo methods have been successfully applied to study the thermodynamic properties.<sup>9,10</sup>

A key insight into the physics can be obtained by studying the spin-correlation function. These functions are very difficult to measure in the interesting low-temperature limit. Manousakis and Salvador<sup>11</sup> (MS) investigated correlation functions of the AFHM on lattices ( $\leq 20 \times 20$ ) by using the Handscomb Monte Carlo method and found that the measured correlation lengths are better fitted by an expression of the Kosterlitz-Thouless (KT) form, which suggests a phase transition induced by topological defects. Gomez-Santos, Joannopoulos, and Negele<sup>9</sup> (GJN) employed an improved variant of the same algorithm, which explores the phase space more efficiently. They measured correlation lengths more accurately, and their results are consistent with the quantum-renormalized classical picture.<sup>6,7</sup> No

evidence of a KT transition was found.

The conflicting signals from these two works may be attributed to the modest range of the correlation lengths measured (from 1 to 4), which is not sufficient to draw quantitative conclusions, since the essential feature of the exponential growth of the correlation length is not evident.

In this Letter we report a systematic study of the Heisenberg antiferromagnet at low temperatures, in order to provide a clear picture of the behavior of the correlation function and to provide a *direct, quantitative* comparison between the Heisenberg model and the experiments on the  $\text{La}_2\text{CuO}_4$  compound.

We have developed a very efficient Monte Carlo algorithm following the Suzuki-Trotter approach.<sup>12</sup> Because of algorithmic advances and usage of a parallel supercomputer, we were able to simulate lattices up to  $128 \times 128$  sites at low temperatures with very high statistics. We give a brief account of the algorithm and the simulation. The details will be reported in Ref. 13. The partition function can be rewritten as

$$Z = \text{Tr} e^{-\beta H} = \text{Tr} (e^{-\beta H/m})^m \\ = \lim_{m \rightarrow \infty} \text{Tr} (e^{-\beta H_1/m} e^{-\beta H_2/m} e^{-\beta H_3/m} e^{-\beta H_4/m})^m, \quad (2)$$

where  $\beta = 1/T$  and  $H = H_1 + H_2 + H_3 + H_4$  is a "bond-type" breakup<sup>12</sup> as shown in Fig. 1. In contrast to the most commonly used "cell-type" breakup,<sup>10,12,14</sup> which leads to eight-spin interactions, the bond-type breakup we use leads to four-spin interactions. This simpler spin interaction has significant advantages in our multispin coding scheme. The Trotter number  $m$  is set to a large integer in a simulation.

After inserting complete sets of states (eigenstates of  $S_i^z$ ), the partition function breaks down into products of Boltzmann factors associated with interacting four-spin plaquettes:

$$\langle S_{i,t}^z S_{j,t}^z | e^{-(\beta J/m) S_i \cdot S_j} | S_{i,t+1}^z S_{j,t+1}^z \rangle, \quad (3)$$

where  $t$  labels the  $4m$  time slices. This becomes a classi-

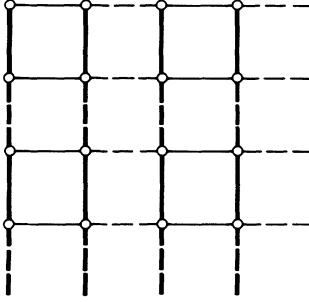


FIG. 1. The bond-type breakup of the Hamiltonian: In the  $x$  direction,  $H_1$  includes bonds indicated by the solid link;  $H_3$ , by the broken link. Similarly for  $H_2$  and  $H_4$  in the  $y$  direction.

cal spin system of general Ising type in 2+1 dimensions. It is then integrated by importance sampling using the standard Metropolis Monte Carlo algorithm. Periodic boundary conditions are imposed in all directions to preserve the translation invariance and to satisfy the trace requirement.

We have designed a set of four elementary updates<sup>13</sup> that can generate all possible spin configurations. Two types of local moves may locally change the spin configurations. A global move in the  $t$  direction changes the magnetization, while another global move in spatial directions changes the winding numbers.

We implemented a simple and very efficient multispin coding method by packing spin lines in the time direction into 32-bit words. Local updates are vectorized. The program runs on a parallel computer by partitioning the 3D lattice into a ring of processor nodes. The local interaction in the system allowed for an efficient parallelization. Parallelism is also achieved by running several independent lattices at the same time. The efficiency of the program is over 90%.

We performed high-statistics simulations on lattice sizes  $32 \times 32$ ,  $64 \times 64$ ,  $96 \times 96$ , and  $128 \times 128$  at  $T/J = 1.0$ , 0.75, 0.60, 0.50, 0.45, 0.35, 0.30, and 0.27. At low  $T$ , we

used a very large  $m = 48$ , which leads to a rather large (2+1)-dimensional spin system:  $128 \times 128 \times 192$ . We did several sufficiently long runs at every  $T$ . For instance, on the  $128 \times 128$  lattice we did two independent runs, each of 298 000 sweeps. The details are summarized in Table I. Finite-size effects in our calculation are very small, since we increase the lattice size to satisfy  $L \geq 6\xi$  at every  $T$ .

We emphasize that the only systematic error in our results is due to the finite value of  $\Delta\tau = 1/mT$ . However, this error is well under control. First, we choose  $m$  large enough to keep  $\Delta\tau \leq 0.07$ . Second, the error is of the order of  $(\Delta\tau)^2$  and is independent of volume because the error terms are proportional to the commutators between  $H_i$ .<sup>12,14,15</sup> At  $T = 0.45J$ , we performed a leading-order  $(\Delta\tau)^2$  extrapolation using the data obtained with  $m = 16$ , 24, and 32. The extrapolated values agree with those of  $m = 32$  well within the statistical errors. In addition, as shown in Table I, at  $T = 0.35J$  on  $64 \times 64$  and at  $T = 0.3J$  on  $96 \times 96$ , we did two simulations: one with  $m = 24$  and the other with  $m = 48$ . The differences between calculated correlation lengths are well within statistical errors.

We measured thermodynamic quantities such as energy, specific heat, etc., and will report them in Ref. 13. Our main focus is to compute the staggered spin-spin correlation function

$$C(r) = (-1)^{r_x+r_y} \frac{4}{L^2} \sum_n \langle S_n^z S_{n+r}^z \rangle \quad (4)$$

at integer distances, where the factor 4 is introduced so that  $C(0) = 1$  and  $L$  is the linear size of the system. At larger  $r$ ,  $C(r)$  has the asymptotic form

$$C_\infty(r) = Ar^{-\lambda} e^{-r/\xi}, \quad (5)$$

where  $\xi$  is the correlation length and  $\lambda$  is the exponent that governs the algebraic part of the correlation function. To incorporate the periodic boundary effects, we fit  $C(r)$  to  $C_L(r) = C_\infty(r) + C_\infty(L-r)$ . The correlation functions at several  $T$  are plotted in Fig. 2 along with the best fits. Clearly, the fits are excellent. The results of

TABLE I. Trotter number, lattice size, number of sweeps, correlation length, and algebraic exponent at various temperatures.

Temperature	$m$	Size	Runs $\times$ sweeps	$\xi$	$\lambda$
1.0	16	$32 \times 32$	$4 \times 100\,000$	0.968(2)	0.36(22)
0.75	24	$32 \times 32$	$4 \times 80\,000$	1.44(2)	0.46(9)
0.6	24	$32 \times 32$	$4 \times 50\,000$	2.20(4)	0.47(3)
0.5	32	$32 \times 32$	$2 \times 50\,000$	3.5(1)	0.51(3)
0.45	16,24,32	$32 \times 32$	$2 \times 130\,000$	4.6(2)	0.46(5)
0.4	40	$64 \times 64$	$4 \times 80\,000$	6.5(2)	0.47(4)
0.35	24	$64 \times 64$	$4 \times 160\,000$	9.9(4)	0.44(6)
0.35	48	$64 \times 64$	$4 \times 130\,000$	10.1(5)	0.36(5)
0.3	24	$96 \times 96$	$4 \times 350\,000$	18.0(5)	0.38(2)
0.3	48	$96 \times 96$	$4 \times 224\,000$	17.5(5)	0.40(2)
0.27	48	$128 \times 128$	$2 \times 298\,000$	28.0(1.2)	0.39(2)

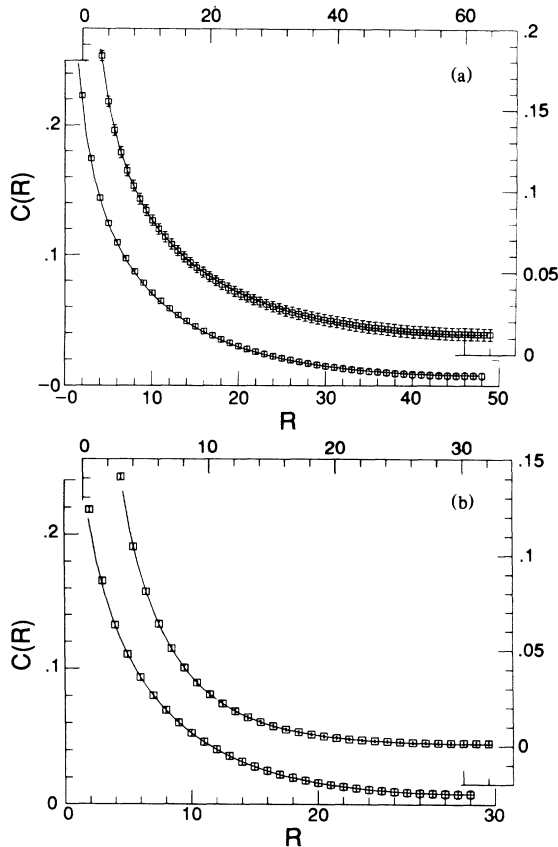


FIG. 2. Correlation functions (squares) and the fit by Eq. (5) (line). (a) Top:  $T=0.27J$  on the  $128 \times 128$  lattice. Bottom:  $T=0.3J$  on  $96 \times 96$ . (b) Top:  $T=0.4J$  on the  $64 \times 64$  lattice. Bottom:  $T=0.35J$  on  $64 \times 64$ .

the fits for  $\xi$  and  $\lambda$  are summarized in Table I.

The semilog plot of the correlation length as a function of  $1/T$  is given in Fig. 3. The data points fall onto a straight line surprisingly well throughout the whole temperature range. This naturally leads to the exponential fitting form:

$$\xi(T) = Ae^{2\pi\rho_s/T}. \quad (6)$$

The fit is indeed very good ( $\chi^2$  per degree of freedom is 0.62), with the parameters of the fit listed in Eq. (7). The KT-type behavior,  $\xi(T) = A \exp[B/(T - T_c)^{1/2}]$ , is clearly ruled out, since it would predict that  $\xi$  grows much faster, diverging at a finite  $T_c$ .

The fitting form given by Eq. (6) is typical of models with  $O(3)$  symmetry in two dimensions. As emphasized by Chakravarty, Halperin, and Nelson<sup>6</sup> (CHN) based on an analysis of the nonlinear  $\sigma$  model, the quantum Heisenberg spins behave qualitatively as the classical ones; only the parameters get multiplicatively renormalized due to quantum fluctuations. Essentially the same result is also obtained by Auerbach and Arovas,<sup>7</sup> who applied Schwinger boson mean-field theory. In particular, the spin stiffness of the antiferromagnet at  $T=0$  is reduced by a factor of  $Z_\xi^S$  from its classical value  $\rho_s = 1$

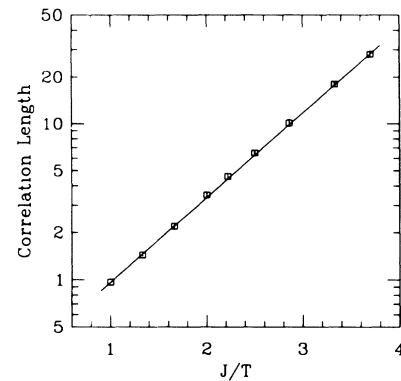


FIG. 3. Correlation length and the fit by Eq. (6). Errors are smaller than the symbol size.

to  $\rho_s = S(S+1)Z_\xi^S$ . [ $S(S+1)$  appears naturally as one goes from the classical spins to quantum spins.] Our data are in complete agreement with their results. The prefactor  $A$  depends on  $T$  in general. In the classical case,  $A \propto T$ . For the nonlinear  $\alpha$  model,<sup>6</sup> at the one-loop level,  $A \propto 1/T$ , while the two-loop calculation yields  $A = \text{const}$ , as in Eq. (6). Note that even though the exponential dominates Eq. (6), the wide range of our data made it possible to clearly distinguish between these different prefactors. Our data show that the prefactor is very close to a constant. In fact, a bound can be set:  $A \propto T^\tau$ ,  $\tau \leq 0.03$ . The excellent fit by Eq. (6) up to  $T \approx 1.0$  indicates that the renormalized classical region is quite wide. This classical picture remains valid up to a crossover temperature where the Josephson and thermal length scales become compatible.<sup>6</sup> In fact, using our measured  $\rho_s = 0.2$  and  $C_p = 0.6$ ,<sup>6</sup> we estimate  $T_{cr} = 0.7$ .

Our best fit with Eq. (6) gives

$$A = 0.276(6), \quad \rho_s = 0.199(2)J \quad [Z_\xi^{1/2} = 0.265(2)]. \quad (7)$$

MS<sup>11</sup> quoted  $\rho_s = 0.22$ . GJN<sup>9</sup> obtained  $\rho_s \approx 0.159$ , about 20% lower than our value. This is partly due to their fitting form being pure exponential, so that their  $\xi$  is systematically smaller than ours. Singh and Huse,<sup>8</sup> using a series expansion around the Ising limit, estimated the spin stiffness constant to be  $\rho_s \approx 0.18(1)$ , in reasonable agreement with our calculation. Auerbach and Arovas<sup>7</sup> determined the quantum renormalization factor to be  $Z_\xi^{1/2} = 0.246$ , quite close to our value. Considering the crudeness of mean-field theory, this is surprising.

The algebraic exponent  $\lambda$  is close to the classical Ornstein-Zernike value of  $\lambda = (d-1)/2 = 1/2$  at higher and medium  $T$ . As  $T$  is lowered,  $\lambda$  appears<sup>13</sup> to deviate slightly from  $1/2$  (see Table I). Note that both the Schwinger boson mean-field theory<sup>7</sup> and Takahashi's<sup>16</sup> variational spin-wave calculation give  $\lambda = 1$ , indicating one of the limits of these approximations.

Recently, extensive neutron-scattering experiments were performed<sup>3</sup> on the undoped superconducting mother compound  $\text{La}_2\text{CuO}_4$ . Correlation lengths of the order of a few hundred Å were measured. Several of our data

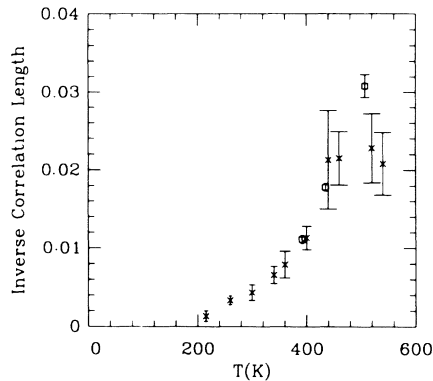


FIG. 4. Inverse correlation length of  $\text{La}_2\text{CuO}_4$  measured in neutron-scattering experiments (Ref. 3), denoted by crosses, and those measured in our simulation, denoted by squares (units in  $(1.178 \text{ \AA})^{-1}$ ).  $J = 1450 \text{ K}$ . At  $T \approx 500 \text{ K}$ ,  $\text{La}_2\text{CuO}_4$  undergoes a structural transition.

points fall within this region, so a direct comparison can be made. The correlation length in our simulation is measured in units of the lattice spacing. The spacing between Cu atoms in a copper-oxygen plane is  $a_H \approx 3.78 \text{ \AA}$ . The only unknown parameter in our calculation is the exchange coupling,  $J$ , which should be set to the correct value. Setting  $J = 1450 \text{ K}$ , in Fig. 4 we plot our data along with those from experiment. The agreement is excellent. This provides strong evidence that the essential magnetic behavior is captured by the Heisenberg model. We emphasize that our simulation is an accurate first-principles calculation, with all possible sources of error under control. Comparing directly with the experiment, we provide an independent determination of the effective exchange coupling:

$$J = 1450 \pm 30 \text{ K}.$$

It is important to compare with other estimates of  $J$ . Raman scattering on these materials<sup>4</sup> exhibits a peak around  $3000 \text{ cm}^{-1}$ . From magnon pairing theory, Lyons and co-workers<sup>4,17</sup> estimated  $J = 1000 \text{ cm}^{-1}$  (or  $1400 \text{ K}$ ). Various moments of the Raman spectrum can be calculated using series expansions.<sup>8,17</sup> By comparing with experiment, Singh *et al.*<sup>17</sup> estimated  $J = 1030 \pm 50 \text{ cm}^{-1}$  ( $1480 \pm 70 \text{ K}$ ). The fact that their estimate is so close to our determination is quite significant. Raman scattering probes the short-wavelength region, where neutron scattering measures the long-range correlations. The agreement of  $J$ 's obtained from these two rather different experiments is another strong indication that the magnetic interactions are dominated by the nearest-neighbor Heisenberg model.

In conclusion, by accurately measuring the correlation functions at low temperatures, we found that the 2D quantum antiferromagnet behaves essentially like a classical system, in good agreement with Refs. 6 and 7.

Direct comparison with the data from neutron-scattering experiments is excellent. This confirms that the magnetic properties of the insulating phase of  $\text{La}_2\text{CuO}_4$  above the 3D Néel ordering temperature are well described by the nearest-neighbor Heisenberg model, and thus leads to a direct determination of the effective exchange coupling:  $J = 1450 \pm 30 \text{ K}$ .

We are indebted to Michael Cross for numerous valuable discussions and to Geoffrey Fox for constant encouragement and support. We thank Peter Weichman, John Preskill, and John Apostolakis for helpful conversations. The calculations were performed on the 32-node Caltech-JPL MarkIIIfp hypercube supercomputer<sup>18</sup> and took about 1000 hours (equivalent to about 1200 Cray XMP hours). This work is supported in part by DOE Grants No. DE-FG0385-ER25009 and No. DE-AC-0381-ER40050 and NSF Grant No. DMR-8715474. M.S.M. acknowledges support from the Shell Foundation.

<sup>1</sup>J. G. Bednorz and K. A. Müller, *Z. Phys. B* **64**, 189 (1986); M. K. Wu *et al.*, *Phys. Rev. Lett.* **58**, 908 (1987).

<sup>2</sup>P. W. Anderson, *Science* **235**, 1196 (1987); T. M. Rice, *Z. Phys. B* **67**, 141 (1987), and references therein.

<sup>3</sup>G. Shirane *et al.*, *Phys. Rev. Lett.* **59**, 1613 (1987); D. Vaknin *et al.*, *Phys. Rev. Lett.* **58**, 2802 (1987); Y. Endoh *et al.*, *Phys. Rev. B* **37**, 7443 (1988).

<sup>4</sup>K. B. Lyons *et al.*, *Phys. Rev. B* **37**, 2353 (1988).

<sup>5</sup>See, for example, I. Affleck, *Phys. Rev. B* **37**, 5186 (1988).

<sup>6</sup>S. Chakravarty, B. I. Halperin, and D. Nelson, *Phys. Rev. Lett.* **60**, 1057 (1988); *Phys. Rev. B* **39**, 2344 (1989).

<sup>7</sup>A. Auerbach and D. P. Arovas, *Phys. Rev. Lett.* **61**, 617 (1988); D. P. Arovas and A. Auerbach, *Phys. Rev. B* **38**, 316 (1988).

<sup>8</sup>R. R. P. Singh, *Phys. Rev. B* **39**, 9760 (1989); R. R. P. Singh and D. A. Huse, *Phys. Rev. B* **40**, 7247 (1989).

<sup>9</sup>D. H. Lee, J. D. Joannopoulos, and J. W. Negele, *Phys. Rev. B* **30**, 1599 (1984); G. Gomez-Santos, J. D. Joannopoulos, and J. W. Negele, *Phys. Rev. B* **39**, 4435 (1989).

<sup>10</sup>S. Miyashita, *J. Phys. Soc. Jpn.* **57**, 1934 (1988); Y. Okabe and M. Kikuchi, *J. Phys. Soc. Jpn.* **57**, 4351 (1988).

<sup>11</sup>E. Manousakis and R. Salvador, *Phys. Rev. Lett.* **60**, 840 (1988); *Phys. Rev. B* **39**, 575 (1989).

<sup>12</sup>M. Suzuki, *Prog. Theor. Phys.* **56**, 1457 (1976); *J. Stat. Phys.* **43**, 833 (1986).

<sup>13</sup>M. S. Makivic and H.-Q. Ding (to be published).

<sup>14</sup>J. E. Hirsch, D. J. Scalapino, R. L. Sugar, and R. Blankenbecler, *Phys. Rev. B* **26**, 5033 (1982).

<sup>15</sup>R. M. Fye, *Phys. Rev. B* **33**, 6271 (1986).

<sup>16</sup>M. Takahashi, *Phys. Rev. B* **40**, 2494 (1989).

<sup>17</sup>R. R. P. Singh, P. A. Fleury, K. B. Lyons, and P. E. Sulewski, *Phys. Rev. Lett.* **62**, 2736 (1989).

<sup>18</sup>For a review of the fast-growing field of parallel computing, see G. C. Fox, *Concurrency: Practice and Experience* **1**, 63 (1989).